Experimental and Numerical Investigation of Concrete-Filled Tube Beams: A Review Paper

Ali M. Abdulridha iD ✉ *, **Salah R. Al Zaidee** iD ✉

Department of Civil Engineering, College of Engineering, University of Baghdad, Baghdad, Iraq

ABSTRACT

Concrete-filled steel tubes (CFST) are structural members consisting of hollow steel tubes filled with concrete. Both steel and concrete work together to provide several advantages. The concrete increases the steel tube's resistance against local buckling while the steel tube confines the concrete, which increases its compressive strength. The use of CFST beams increased in high buildings due to their great mechanical properties. The researchers were interested in CFST beams because of their great ductility, stiffness, strength, and flexural capacity when compared to hollow steel beams. The properties of CFST beams were enhanced in several ways, for example, by using carbon fiber reinforced polymer (CFRP) wrapping, adding an external steel plate, and using recycled aggregate. In addition, the concrete properties were improved by adding steel and synthetic fibers. This review paper covers research conducted on CFST beams since 2019. It gives an overview of what was studied and explored and what still needs more research.

Keywords: Concrete-filled steel tubes, CFST, Composite beam, Confinement, Failure mode.

1. INTRODUCTION

The use of composite structures provides more efficient and economical solutions than using the material separately. A composite material refers to the use of two or more materials to create one unique element with several benefits compared to non-composite elements **(Fahmi and Tofeq, 2012; Mohammed and Mohsen, 2014; Ibrahim et al., 2019)**. Concrete-filled steel tubes (CFST) are composite members when the concrete is used to fill the hollow steel tube to improve its mechanical properties, see **Figure 1**. It combines the excellent compressive strength of concrete and the great flexural strength of steel **(Prion and Boehme, 1994; Chen et al., 2020; Zhou et al., 2023)**, which enhances the ability of the structure to deform. The filling concrete increases the steel tube's resistance against the global buckling and limits the local buckling, which improves the compressive strength of concrete due to the confinement effect **(Alshimmeri, 2016; Du et al., 2019)**. The steel tubes may be filled partially with concrete **(Nguyen et al., 2023)**.
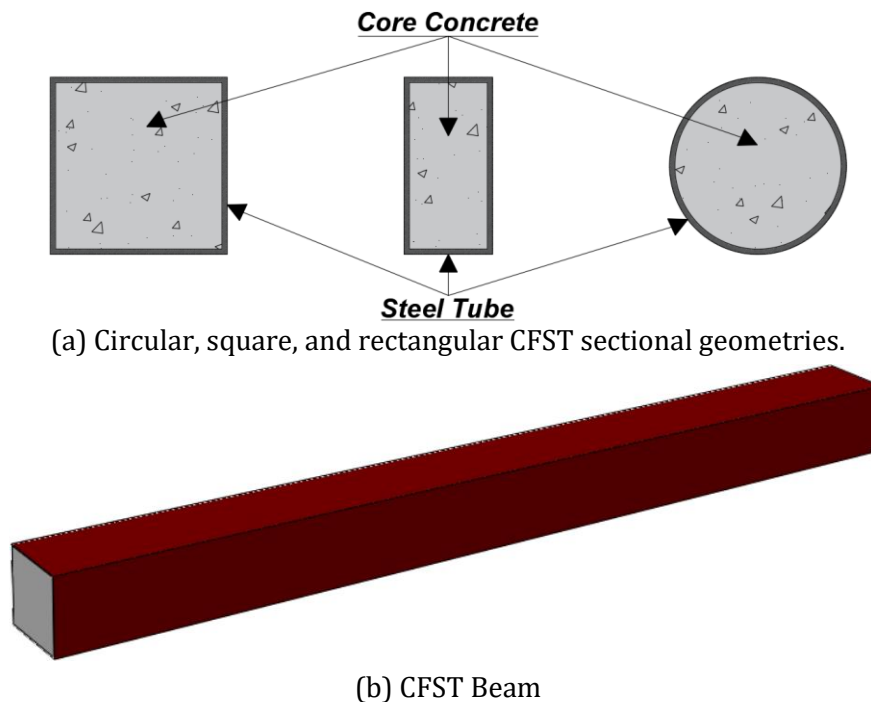
(a) Circular, square, and rectangular CFST sectional geometries.

(b) CFST Beam

Figure 1. (a) CFST sections and (b) Beam representation.

CFST columns were used widely in high-rise buildings, bridges, structures designed to withstand seismic loads, railway decks, and for supporting storage tanks due to their high ductility, ability to support heavy loads, and excellent fire resistance **(Wang et al., 2009; Aziz et al., 2016; Li et al., 2021; Hassooni and Al Zaidee, 2022)**. Recently, research performed on CFST members under pure bending showed that CFST beams have high ductility, fire resistance, stiffness, strength, flexural, and energy absorption compared to hollow steel tubes. Furthermore, steel tubes can be used as formwork during construction **(Han et al., 2014; Flor et al., 2017; Alqarni et al., 2019; Zhang et al., 2022a; Alghossoon and Varma, 2023)**.

CFST beams can be enhanced using different methods. One of these methods is using carbon fiber reinforced polymer (CFRP) sheets to wrap CFST beams to increase their strength. CFRPs are lightweight, have excellent resistance to corrosion, are not affected by high temperatures, remain undamaged by ultraviolet rays, and can be easily shaped to fit different parts. They also have great fatigue strength because they do not absorb water **(Al Zand et al., 2018; Du et al., 2023; Ou et al., 2023)**. CFST beams can be improved by adding a steel plate on the tension side. It is an economical method that enhances ductility and stiffness and increases moment-carrying capacity **(AL-Shaar and Göğüş, 2018)**. Welding round steel with different diameters on the tension side of the tube was investigated by **(Liu et al., 2019; Liu et al., 2021)** to increase the flexural failure resistance of the CFST beam.

Using recycled or waste materials as recycled aggregate is an accepted method. It aims to reduce the environmental impact and support sustainable construction **(Arivalagan and Kandasamy, 2010b; Ghannam, 2016; Xu et al., 2020)**. Rubberized concrete (Rcu) when rubber aggregate is used instead of coarse natural aggregate, is not only a safe, environmentally friendly, and economical way to recycle the millions of waste tires produced annually but also enhances ductility, energy absorption, fracture toughness, seismic resistance, and changes the failure behavior compared to normal concrete (NC) **(Dong et al., 2019a; 2019b)**.

The use of sawdust, which is a waste product generated by the wood and timber industries, as a lightweight aggregate has enhanced lightweight concrete. Using sawdust waste achieved a noticeable reduction in the thermal conductivity of the cement composite by up to 20%. Replacing 25% or more of natural aggregates with sawdust can negatively affect the mechanical characteristics and density of the concrete **(Hanoon et al., 2023)**. Demolished concrete lumps (DCLs) resulting from the demolition of old buildings can be recycled to produce reused aggregates. The application of DCLs in structural elements has been greatly limited because their properties are not as good as those of natural aggregates. The concrete developed a notable increase in harmful pores, and as the percentage of DCL replacement increased, the compressive strength of the concrete decreased **(Khalaf et al., 2023)**.

The tensile strength of normal concrete is considerably less than its compressive strength, leading it to exhibit a brittle response when subjected to tensile forces. Lately, the concrete has been improved by adding different types of steel and synthetic fibers, which improves the concrete's ductility and toughness characteristics. While microfibers in concrete limit small cracks during the early stages, macro fibers significantly improve its behavior as it nears failure **(Guler and Yavuz, 2019).**

The aim of this review paper is to summarize the most recent research on concrete-filled tube beams conducted from 2019 onwards. The properties of CFST beams, including load-carrying capacity, ductility, failure modes, and other factors, were studied. The summary provides an overview of what has been studied and discovered and the gaps or areas that need to be filled.

2. CONCRETE-FILLED TUBE BEAM

This term refers to structural elements made of hollow tubes that are filled with concrete **(Han, 2004; Joseph et al., 2016)**, or it may consist of a double-skin tube where there is an interior smaller section, and the concrete lays between the two sections, to reduce weight, and improve seismic performance **(Eom et al., 2019; Li et al., 2020)**. There are several types of filled tube beams depending on the material that the tube is made of, such as Steel-filled tube beams, where the steel serves as the confinement element, and the tube is filled with concrete **(Hou et al., 2016; Saini and Shafei, 2019)**. There are glass fiber-reinforced polymer tubes (GFRP), where (FRP) materials offer a notable benefit in improving fatigue characteristics **(Aslani et al., 2019; Abdeldaim et al., 2020)**. Another type of confinement material is aluminum cross sections, which are used to get lightweight sections with excellent corrosion properties **(Gkantou et al., 2023)**.

3. MATERIALS AND SPECIMEN DETAILS

The following sections extensively focus on materials and their characteristics. Comprehensive information about these materials is provided by tables describing geometric configurations and dimensions under consideration. Only the main materials (steel and concrete) are considered here and the other additional materials are mentioned as needed.

3.1 Material Properties

3.1.1 Steel

Known for its isotropic nature, steel exhibits consistent stress and strain responses in both tension and compression zones **(Al Zand et al., 2020)**. There has been increasing use of

stainless steel as a tube material because it offers several advantages, including an attractive appearance, remarkable durability, exceptional fatigue corrosion resistance, ease of maintenance, and heightened fire resistance **(Chen et al., 2017; Feng et al., 2018)**. Consequently, this paper includes specimens of stainless-steel tubes. **Table 1.** shows an overview of the tube materials used and their key properties.

Table 1. Steel tubes' properties.

Yield Strength (MPa)	ultimate strength (MPa)	Elastic modulus (GPa)	Notes	Reference
345	-	200	-	**(Nimisha and Abhilasha, 2019)**
350	430	-	-	**(Dong et al., 2019b)**
245	530	-	-	**(Liu et al., 2019)**
350	430	-	-	**(Dong et al., 2019a)**
390	433	-	Square tube	**(Farhan and Shallal, 2020)**
305	391	-	Circular tube	
270	410	205	-	**(Chavan et al., 2021)**
731.9	813.9	205.792	-	**(Du et al., 2023)**
277, 257	355, 307	-	C1, C2	**(Khalaf et al., 2023)**
364.1	430.8	201	-	**(Ou et al., 2023)**
385	483	-	Outer steel tube	**(Al-Nini et al., 2020)**
401	421	-	Inner steel tube	
230, 227, 234, 282, 276, 290	286, 278, 304, 512, 504, 526	186, 180, 192, 198, 192, 201	CS 2, 3, 4 mm SS 2, 3, 4 mm	**(Guler and Yavuz, 2019)**
318.5	507.1	206	-	**(Wu et al., 2019)**
250.7	400	200	-	**(Hanoon et al., 2023)**
345	715.3	212	Stainless steel	**(Dabbagh et al., 2023)**
250	-	-	-	**(Pandian and Narayanan, 2023)**
355	-	-	-	**(Shi et al., 2020)**
420, 406, 400, 429	603, 589 592, 587	205, 206 206, 205	4.5, 6, 8, 10 mm thickness.	**(Wu et al., 2021)**
-	-	-	-	**(Karuppanan and Vennila, 2020)**
297	388	200	-	**(Mujdeci et al., 2022)**
741	795	201.5	-	**(Zhang et al., 2022b)**
346	432	198.2	-	**(Al Zand et al., 2020)**
489	558	201	-	**(Al Zand et al., 2021)**
430.3	573.8	-	-	**(Tahir and Shallal, 2021)**
365	397.5	-	-	**(Mahdi and Shallal, 2021)**

3.1.2 Concrete

The widespread use of concrete in construction arises from the abundant availability of raw materials and its capacity to be molded into various sizes, shapes, and colors with ease **(Hanoon et al., 2018)**. It is widely used as a filling material for steel tubes. It may be normal concrete (NC) **(Lu et al., 2009)**, high-strength concrete **(Xiong et al., 2017)**, lightweight concrete (LWC) **(Assi et al., 2003)**, or concrete with some additional materials. For example, the fine and coarse aggregates can be replaced with different rates of materials, such as rubber replacement **(Abuzaid et al., 2019; Mujdeci et al., 2021; Elghazouli et al., 2022)**, quarry waste concrete **(Arivalagan and Kandasamy, 2010a)** or by using Demolished

Concrete Lumps (DCLs), which are Produced by crushing concrete to recycle concrete **(Yang et al., 2015; Khalaf et al., 2023)**. One of the most common materials added to concrete is fiber, such as steel fiber **(Dexin, 2012)**. The concrete may be reinforced with longitudinal bars **(Brown et al., 2015)**, prestressed concrete **(Deng et al., 2013; Zhan et al., 2016)** or reinforced concrete with steel sections **(Xian et al., 2020; Zhu et al., 2021)**. **Table 2** shows an overview of the concrete used and its key properties.

Table 2. Concrete properties.

Compressive Strength (MPa)	Notes	Reference
30	Fcu, varying compressive strengths used.	**(Nimisha and Abhilasha, 2019)**
40.8, 17.9, 9.5	f_c', NC, RuC15 (15%), and RuC30 (30% rubber), respectively.	**(Dong et al., 2019b)**
40	Fcu	**(Liu et al., 2019)**
40.8, 17.9, 9.5	f_c', NC, RuC15 (15%), and RuC30 (30% rubber), respectively.	**(Dong et al., 2019a)**
21.85	Fcu, LWC	**(Farhan and Shallal, 2020)**
25	Fcu	**(Chavan et al., 2021)**
62.8, 128.2	Fcu	**(Du et al., 2023)**
28, 36	f_c', Fcu	**(Khalaf et al., 2023)**
40.6	Fcu	**(Ou et al., 2023)**
92.96, 103.89, 108.03	Fcu, Mix A, B, and C, respectively.	**(Al-Nini et al., 2020)**
35.6, 74.8	Fcu	**(Guler and Yavuz, 2019)**
141.5, 119.2	Average of 3 cubes and 3 prisms, respectively.	**(Wu et al., 2019)**
32.47, 30.11, 28.62, 25.86, 24.06, 22.85	f_c', CFST0 (0%), CFST5 (5%), CFST15 (15%), CFST25 (25%), CFST35 (35%), and CFST45 (45% sawdust), respectively.	**(Hanoon et al., 2023)**
27.8, 24.3, 20.9	Fcu, MC0 (0%), MC50 (50%), and MC100 (100% recycled aggregate), respectively.	**(Dabbbagh et al., 2023a)**
24.2, 27.74, 32.97	Fcu, M20, M25, M30, respectively.	**(Pandian and Narayanan, 2023)**
50	Fcu	**(Shi et al., 2020)**
113, 117, 139, 126	Fcu, C20, C30, C32, C02	**(Wu et al., 2021)**
53.1	Fcu, varying compressive strengths used.	**(Karuppanan and Vennila, 2020)**
70.7, 18.1, 6.2	Fcu, NC, R30 (30%), R60 (60% rubber), respectively.	**(Mujdeci et al., 2022)**
51.2	Fcu	**(Zhang et al., 2022b)**
45.1	Fcu	**(Al Zand et al., 2020)**
26.2, 14.6, 14.1, 13.7	Fcu, RC0 (0%), RC30 (30%), RC50 (50%), and RC70 (70% recycled aggregate), respectively.	**(Al Zand et al., 2021)**
23.08, 46.67, 56.95	Fcu, LWC, NC, NC, respectively.	**(Tahir and Shallal, 2021)**
17.38, 38.27	Fcu, LWC and NC, respectively.	**(Mahdi and Shallal, 2021)**

3.2 Geometry and Test Specimens

Table 3. contains the most important details about the physical aspects of the experiments conducted in the previous studies, which are considered in this review. It includes information about the size, shape, and characteristics of the objects (test specimens) used.

Table 3. Geometry and specimens' properties.

| Geometry	Number of Specimens	cross-section (mm)	Thickness (mm)	Length (mm)	Notes	Reference
Square	3	-	2	1000	Varied cross-section dimensions used.	**(Nimisha and Abhilasha, 2019)**
Square	8 8	89×89 100×100	-	1000	Varied tube thicknesses used.	**(Dong et al., 2019b)**
Circular	6	194	10	2820	-	**(Liu et al., 2019)**
Circular	8 8	88.9 114.3	-	1000	Varied tube thicknesses used.	**(Dong et al., 2019a)**
Square Circular	7 2	150×150 150	4 3.8	- 1800	Varied square beam lengths used.	**(Farhan and Shallal, 2020)**
Rectangular	12	96×48	3.2	1000	-	**(Chavan et al., 2021)**
Square	6	200×200	3	1800	-	**(Du et al., 2023)**
Circular	16	219	-	1500	C1 (4 mm) and C2 (5 mm) thick.	**(Khalaf et al., 2023)**
Circular	9	114	2.9	1300	-	**(Ou et al., 2023)**
Rectangular	8	100×75 65×35	2.3 2.3	1500 1500	Outer tube dimensions Inner tube dimensions	**(Al-Nini et al., 2020)**
Square	66	100×100	-	1000	Varied tube thicknesses used.	**(Guler and Yavuz, 2019)**
Circular	3	203	6	2000	-	**(Wu et al., 2019)**
Rectangular	6	160×80	3	1500	-	**(Hanoon et al., 2023)**
Rectangular	6	100×150	3	1800	-	**(Dabbagh et al., 2023)**
Square	7	92×92	3.2	1100	-	**(Pandian and Narayanan, 2023)**
Circular	6	220	4.4	1940	-	**(Shi et al., 2020)**
Circular	7	114	-	1400	Varied tube thicknesses used.	**(Wu et al., 2021)**
Square	12	110×110	-	1500	-	**(Karuppanan and Vennila, 2020)**
Circular	8	152	2.8	-	Varied beam lengths used.	**(Mujdeci et al., 2022)**
Circular	15	-	2	1800	Varied diameters used.	**(Zhang et al., 2022b)**
Square	6	200×200	1.5	-	Varied beam lengths used.	**(Al Zand et al., 2020)**
Rectangular	25	200×150	1.5	2800	-	**(Al Zand et al., 2021)**
Square	7	160×160	3	-	Varied beam lengths used.	**(Tahir and Shallal, 2021)**
Square	3	100×100	3	1500	-	**(Mahdi and Shallal, 2021)**

4. RESULTS AND DISCUSSION

4.1 Effect of Geometry on CFST Beams

Previous research studied the effect of various geometric configurations on the behavior of concrete-filled steel tube beams. Here, changes in shape and dimensions are explored in terms of how they affect the performance and structural characteristics of CFST beams.

4.1.1 Effect of D/t ratio

(Nimisha and Abhilasha, 2019; Wu et al., 2021) investigated the effect of depth-to-thickness ratio by changing the thickness of steel tubes. The conclusion from the research was that the moment-carrying capacity increases due to D/t ratio decreasing. This was also investigated by **(Al Zand et al., 2020)** and **(Al Zand et al., 2021)** using FE analysis. For example, the ultimate moment capacity increased to 79.7% and 150% for the SB2-SV specimen when the thickness increased from 1.5 mm to 3 mm and 4.5 mm, respectively. Additionally, for the control model, it increased by 30.6% and 60.3% when the thickness went up from 1.5 mm to 2 mm and 2.5 mm, respectively, where SB (short span), LB (long span), SV (single V), and DV (double V), C (control specimen). Stainless steel followed the same trend, with increased tube thickness leading to a more compact section. For instance, as the D/t ratio decreased from 48 (slender) to 15 (compact), the ultimate moment (Mu) value increased by about 242% **(Dabbagh et al., 2023)**. By using Finite Element Analysis for tube thickness between 1 mm and 5 mm, while the other properties remained unchanged, **(Hanoon et al., 2023)** showed a consistent reduction in the buckling failure of the upper flange when the tube thickness exceeded 2 mm. Furthermore, the thicker tubes became much stiffer. **Figure 2** illustrates how the D/t ratio influences beam capacity.
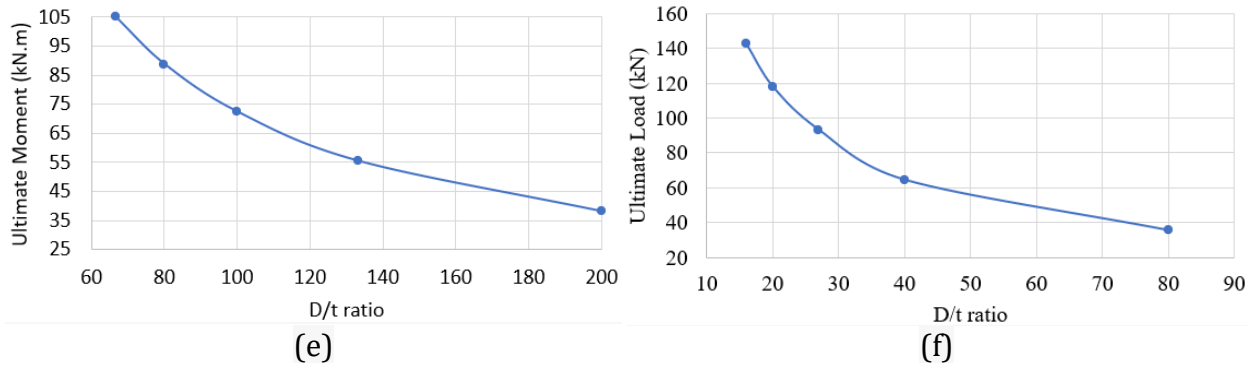

(a)

(b)

(c)

(d)

(e)　　　　　　　　　　　　　　　(f)
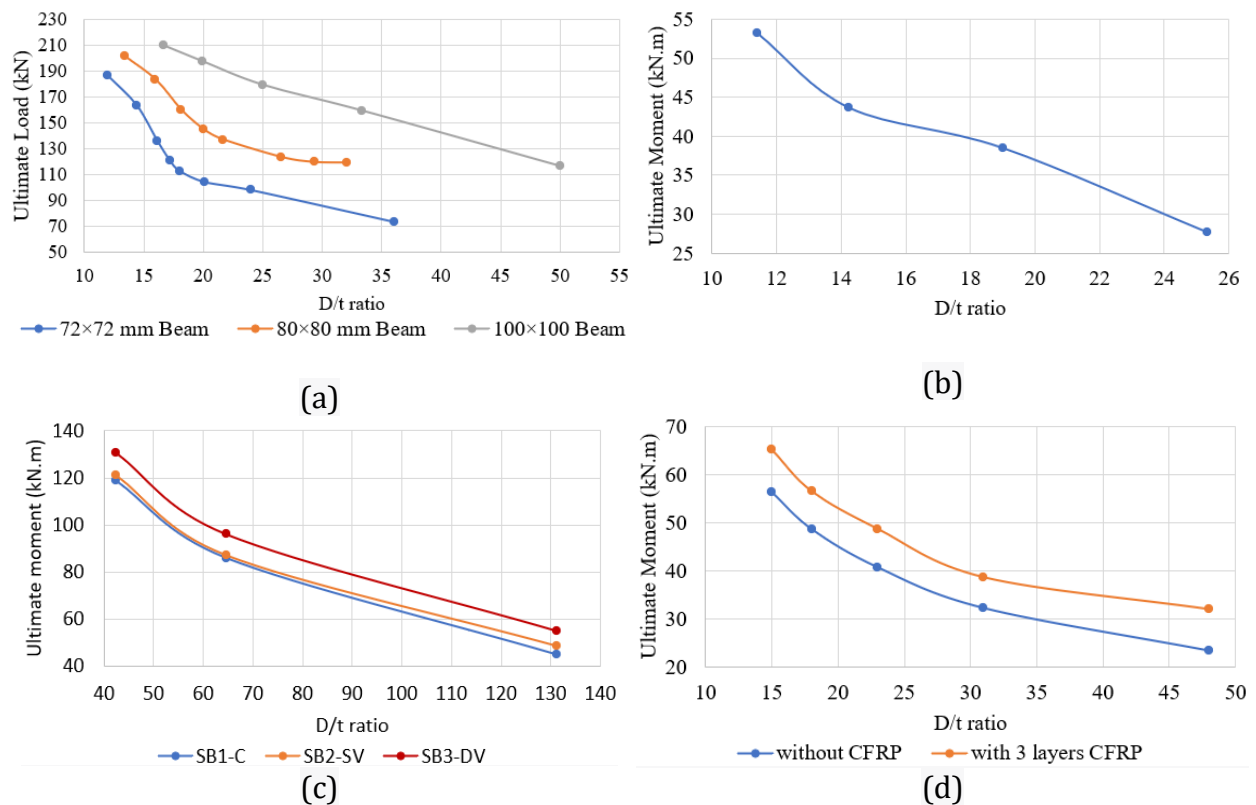
Figure 2. Ultimate moment and load capacity with D/t ratio, **(a) (Nimisha and Abhilasha, 2019) (b) (Wu et al., 2019) (c) (Al Zand et al., 2020) (d) (Dabbagh et al., 2023) (e) (Al Zand et al., 2021) (f) (Hanoon et al., 2023).**

4.1.2 Effect of L/D ratio

The load capacity decreases for CFST beams with the increase in the L/D ratio **(Nimisha and Abhilasha, 2019; Farhan and Shallal, 2020; Tahir and Shallal, 2021)**. **(Al Zand et al., 2021)** confirmed these findings, highlighting the impact of decreasing the L/D ratio on the increase in moment-carrying capacity value. **Figure 3** shows how the L/D ratio influences beam capacity.

(a)　　　　　　　　　　　　　　　(b)

(c)　　　　　　　　　　　　　　　(d)
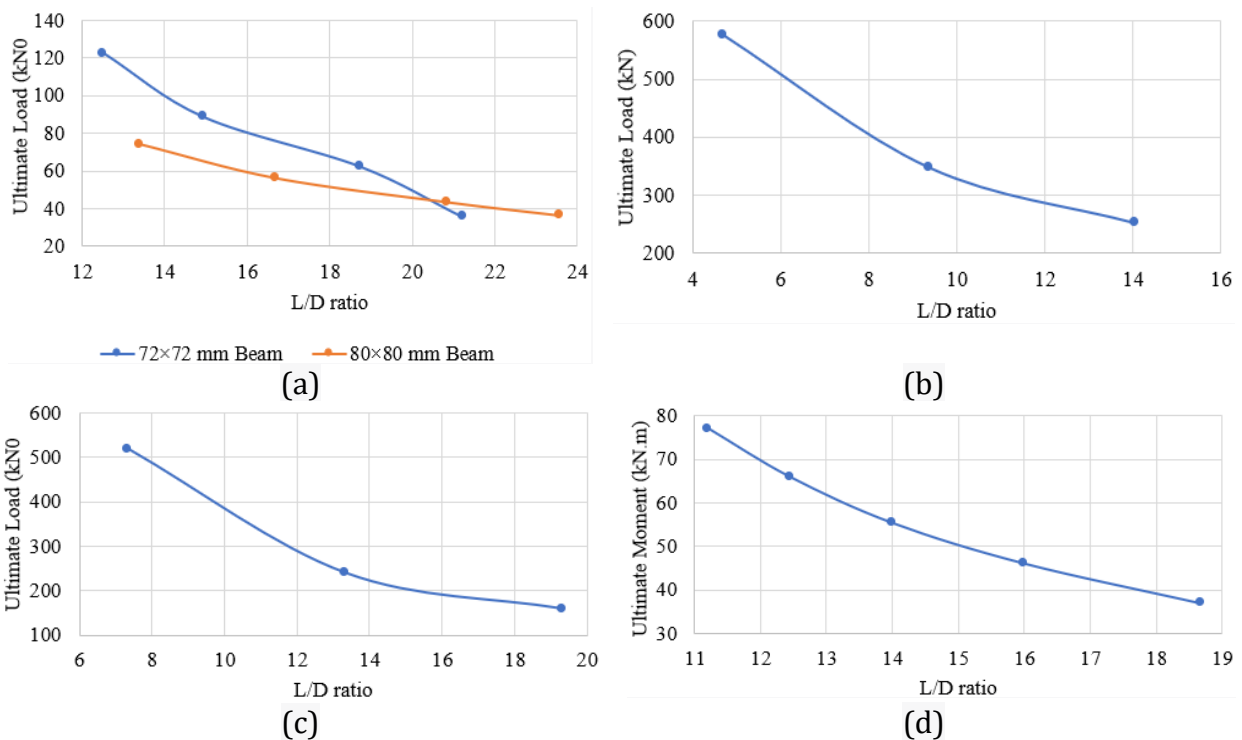
Figure 3. Ultimate moment and load capacity with L/D ratio, **(a) (Nimisha and Abhilasha, 2019) (b) (Tahir and Shallal, 2021) (c) (Farhan and Shallal, 2020) (d) (Al Zand et al., 2021).**

4.1.3 Effect of shape of CFST section

CFST beams are influenced by cross-section shape. **(Nimisha and Abhilasha, 2019)** found that square CFST beams exhibit superior confinement effectiveness and load-carrying capacity compared to rectangular CFST beams. **(Farhan and Shallal, 2020)** showed that the ultimate load for beams with square sections S20-35-2000 and S20-55-2000 increased by 14.8% and 13.4% compared to the circular sections C20-35-2000 and C20-55-2000, respectively. The behavior of the load-deflection curve using different cross-section shapes is presented in **Figure 4** below.
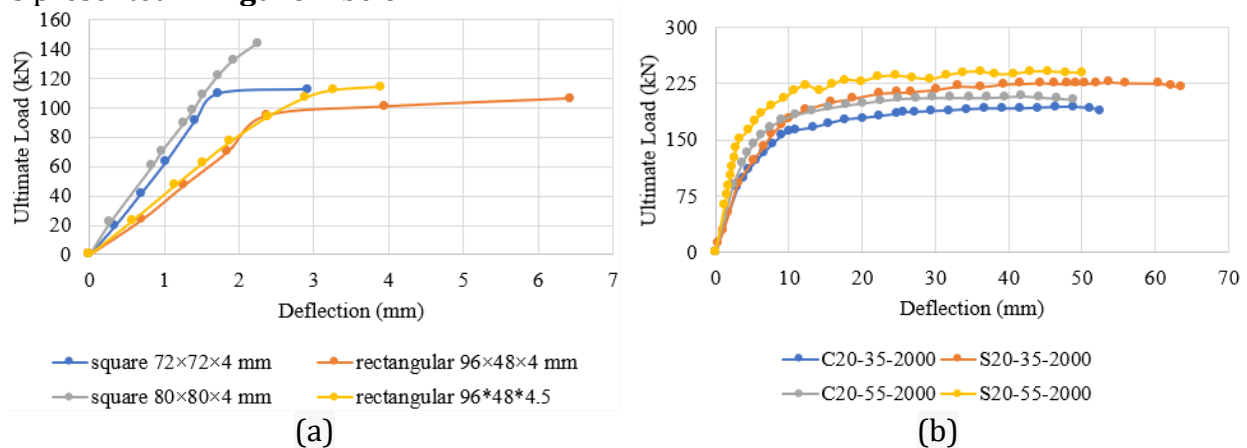
Figure 4. Effect of cross-section shape on load-deflection curve, **(a) (Nimisha and Abhilasha, 2019) (b) (Farhan and Shallal, 2020).**

4.2 Effect of Compressive Strength of Concrete

Increasing concrete compressive strength enhanced the strength of CFST beams and improved ultimate load-carrying capacity **(Nimisha and Abhilasha, 2019; Shi et al., 2020; Al Zand et al., 2021; Tahir and Shallal, 2021; Zhang et al., 2022b; Pandian and Narayanan, 2023)**. For example, when the compressive strength increased from 17.38 MPa to 38.27 MPa, the ultimate load capacity increased from 82.5 kN to 95.5 kN **(Mahdi and Shallal, 2021)**. The same trend was observed by **(Al Zand et al., 2020)** using a finite element model, as illustrated in **Figure 5**, where SB (short span), LB (long span), SV (single V), and DV (double V), C (control specimen).

Research by **(Dong et al., 2019a; 2019b)** explored rubber as an aggregate replacement, revealing a decrease in compressive strength with higher rubber content. For instance, at 15% rubber replacement, strength decreased by 56%, and at 30%, it decreased by 77%, there by impacting the ultimate load-carrying capacity. The same results were achieved by **(Mujdeci et al., 2022)** when using 30% and 60% rubber as aggregate replacements. Additionally, the inclusion of steel fiber in the concrete mixture, as per **(Al-Nini et al., 2020; Karuppanan and Vennila, 2020)**, increased CFST beam strengths. (Guler and Yavuz, 2019) found that increasing compressive strength from 30 MPa to 70 MPa led to a more significant improvement in ductility compared to moment capacity. **Figure 5** shows the relation between the compressive strength of concrete and the ultimate load capacity increase.
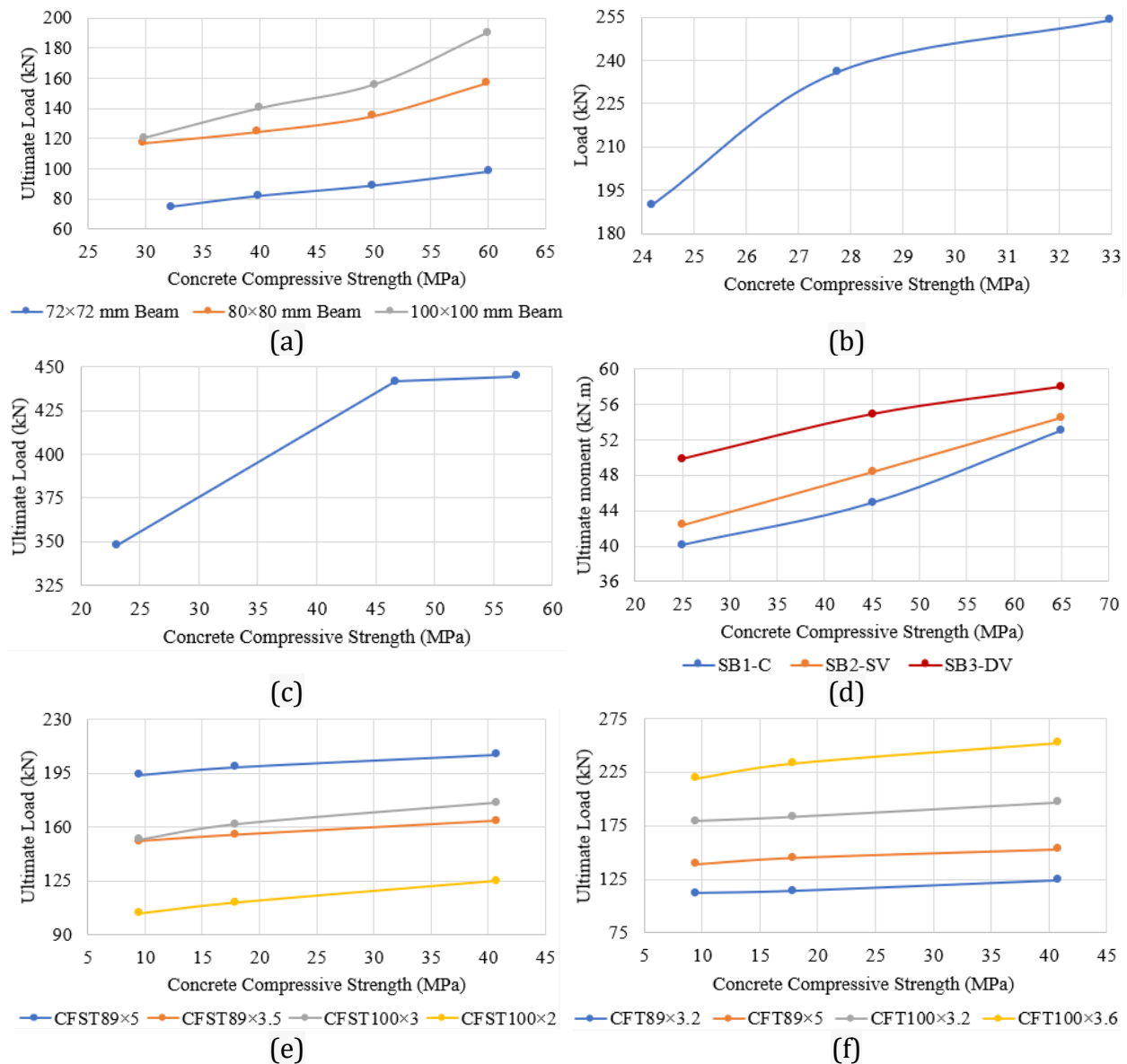
Figure 5. Effect of concrete compressive strength on ultimate load capacity, **(a) (Nimisha and Abhilasha, 2019) (b) (Pandian and Narayanan, 2023) (c) (Tahir and Shallal, 2021) (d) (Al Zand et al., 2020) (e) (Dong et al., 2019b) (f) (Dong et al., 2019a).**

4.3 Failure Mode

In a CFST beam test to investigate failure modes, vertical displacement reached its highest point at the beam center, revealing local buckling and plastic deformations on upper flanges. A common pattern observed was crushed concrete in the compression zone with tension-induced cracks on the beam's underside **(Wu et al., 2019; Tahir and Shallal, 2021; Zhang et al., 2022b)**. In the control beam, cracks appeared at mid-height with widths ranging from 2 to 4 mm. Beams strengthened with welded round steel showed narrower additional cracks, suggesting welded steel significantly minimized crack formation **(Liu et al., 2019)**. **(Wu et al., 2021)** showed that adding steel fibers to the filling concrete minimizes crack formation. Without steel fibers, the compression side of the core concrete fractured into blocks, while with 2% steel fibers, only limited small cracks were observed. By incorporating

rubber replacements up to 60%, the cracks became narrower and denser, resulting in shorter crack lengths compared to 0% and 30% replacements **(Mujdeci et al., 2022)**.

(Du et al., 2023; Al-Nini et al., 2020) found that the deflection shape remained consistent, whether the beam had CFRP sheets or not. At about half of the ultimate bearing capacity, a faint sound of resin delamination occurred. At 80-90%, transverse CFRP sheets on the tension side cracked and broke. At full load, part of the longitudinal CFRP sheets in the mid-span cracked with a loud noise, resulting in buckling. No slip failure was observed between the steel tube and concrete, indicating a strong bond **(Al Zand et al., 2021; Mahdi and Shallal, 2021)**. CFRP-wrapped beams with circular sections exhibited two common failure modes, debonding and fracture of CFRP **(Ou et al., 2023)**.

(Khalaf et al., 2023) studied CFST beams with partially incorporated demolished concrete lumps. The reference beam, beam with inner DCLs, and inner-free beams failed similarly without local buckling on the upper side. For ultra-high-performance cementitious composites filled steel tubes (UHPCC-FST) beams had flexural deformation with plastic hinges in the impact zone. Even with high-performance fiber-reinforced cementitious composite-filled double-skin steel tubes (HPCFDST), beams had the same deflection shape before reaching ultimate strength **(Al-Nini et al., 2020)**. Delamination issues at CFRP ends were seen in specimens with 50% wrapped lengths but avoided in those with 75% wrapped lengths. Specimens with 75% wrapped lengths failed steadily due to CFRP rupture.

(Guler and Yavuz, 2019) observed that 3 mm and 4 mm steel tube thickness led to a greater number of local buckles than beams with 2 mm thickness. Local buckling caused failure in hollow specimens, while overall flexural buckling in filled beams, especially with 3 mm and 4 mm thickness, caused failure. Despite an increase in concrete compressive strength from 30 to 70 MPa, the local buckle number remained constant. In specimens with Sawdust replacement, noticeable buckling of top flanges occurred at 75–85% of ultimate capacities **(Hanoon et al., 2023)** and at 70–80% of ultimate capacities for internally stiffened specimens **(Al Zand et al., 2021)**. **(Al Zand et al., 2020)** observed similar trends in control specimens, while with a single V-shaped groove, specimens buckled outward at around 85% of ultimate capacity. In double V-shaped groove specimens, there was no buckling between two-point loads, with less pronounced failure under these loads compared to similar specimens. The short specimens exhibited outward deformation and longitudinal core slipping at ultimate capacity, unlike longer-span specimens.

The failure mode and deflection shape were consistent for beams with different recycled aggregates. Beams with 0% and 100% recycled aggregate exhibited similar failure patterns. However, MC100 showed greater damage under point loads than MC0 due to decreased compressive strength **(Dabbagh et al., 2023)**. All beams exhibited ductile failure, without any tension fractures noted in the top flange, as reported by **(Pandian and Narayanan, 2023)**. An excellent post-yield behavior was demonstrated by the specimens. The failure of beams involved significant deflection, with no horizontal displacements or other instabilities noted. The failure mode was the same even when the concrete was reinforced with I- or cruciform-section steel **(Shi et al., 2020)**.

4.4 Load and Moment-Carrying Capacity

When the hollow tube was filled with concrete, the moment-carrying and load-carrying capacity increased **(Chavan et al., 2021; Pandian and Narayanan, 2023)**. Even though there was a 409% increase, **(Al Zand et al., 2021)** found that this enhancement was reduced

when recycled aggregate was used. When rubber is used as a replacement material for aggregate, it tends to reduce the compressive strength of concrete. However, the RuCFST beams experienced only a minor average reduction in strength, primarily due to the limited impact of concrete strength. Therefore, RuC was found to be an effective choice as the concrete infill in CFST systems **(Dong et al., 2019b; 2019a; Mujdeci et al., 2022)**.

Strengthening beams with CFRP layers increased moment capacity. Specimen, with two CFRP layers covering 75% of its length, showed a capacity increase of 25% close to the fully covered beam's increase (26%) **(Al-Nini et al., 2020)**, where F for (fully wrapped), P for (partially wrapped), the number after the for (percentage of wrapping), and L (number of CFRP layers). Similar results were observed when using high-strength core concrete **(Du et al., 2023)**. Using steel and hybrid fibers had a minimal effect on increasing the moment capacities, which were slightly increased by increasing the compressive strength of concrete **(Wu et al., 2021)**. For 30 MPa concrete, increases were 70.2% and 46% for carbon steel (CC) and stainless steel (SS), respectively, and 88.2% and 79.1%, respectively, for 70 MPa compressive strength **(Guler and Yavuz, 2019)**. However, the inclusion of polypropylene fiber did not result in an increase in load-carrying capacity, with the capacity remaining almost the same **(Karuppanan and Vennila, 2020)**.

Specimens with recycled aggregate incorporating sawdust had lower moment values due to decreased compressive strength yet achieved loading performance similar to conventional concrete specimens **(Hanoon et al., 2023)**. The same behavior was observed with stainless steel tubes and different recycled aggregates **(Dabbagh et al., 2023)**. For the reinforced concrete with steel sections, major-axis loaded beams have slightly greater moment capacity due to their larger moment of inertia compared to minor-axis loaded beams. When comparing different profiled steel shapes with the same ratio, I-section steel showed slightly higher moment capacity than cruciform steel when loaded along the major axis **(Shi et al., 2020)**, where (CI) refers to beams reinforced with I-section and (CC) for beams with cruciform-section while (S) for strong axis and (W) for weak axis of I-section, used in **Figure 6**. **(Al Zand et al., 2020)** found that double V-shaped grooves beams resulted in higher Mu values compared to their corresponding beams. **Figure 6** shows the moment and load capacity variation with different effects.
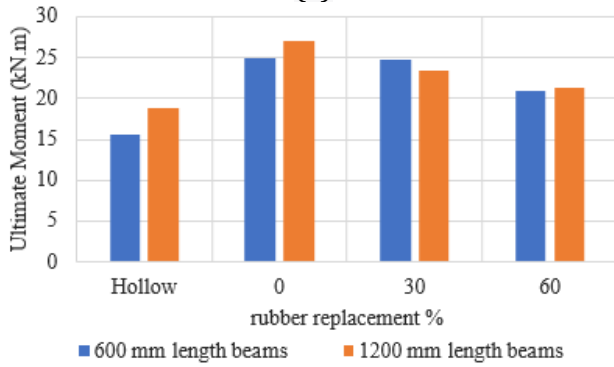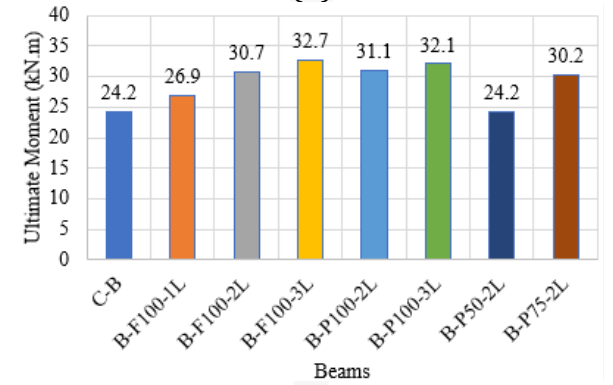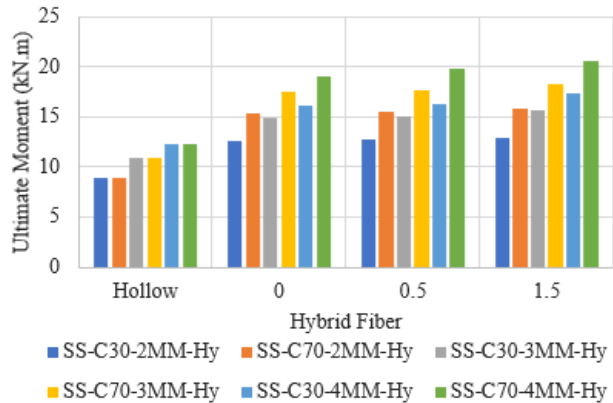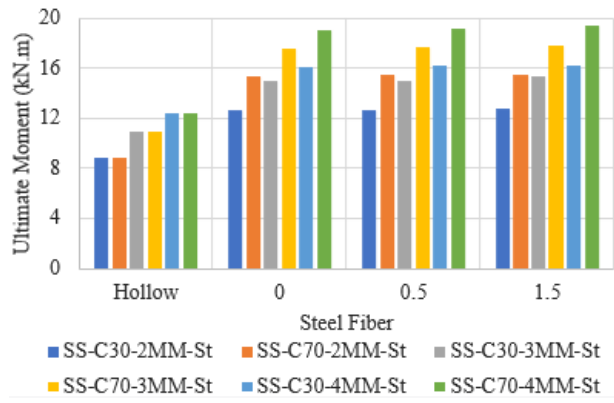

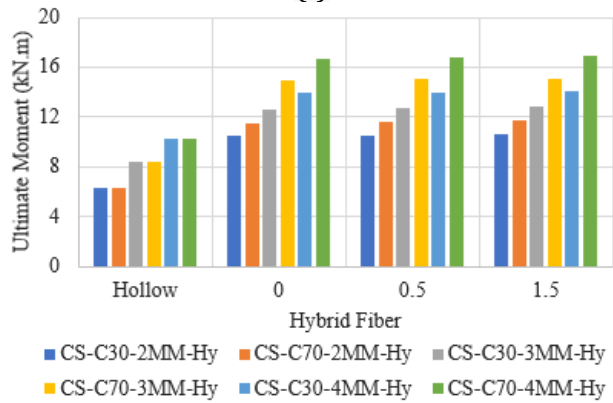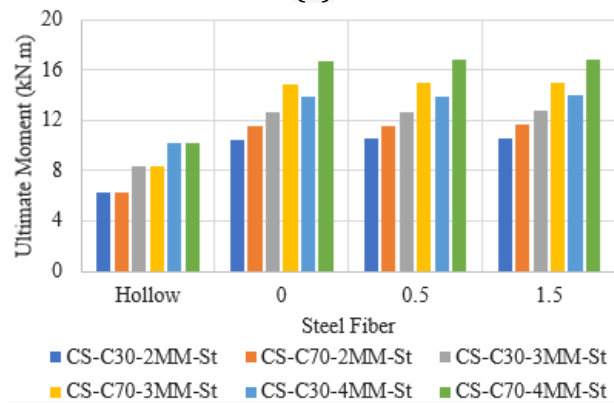(a)   (b)
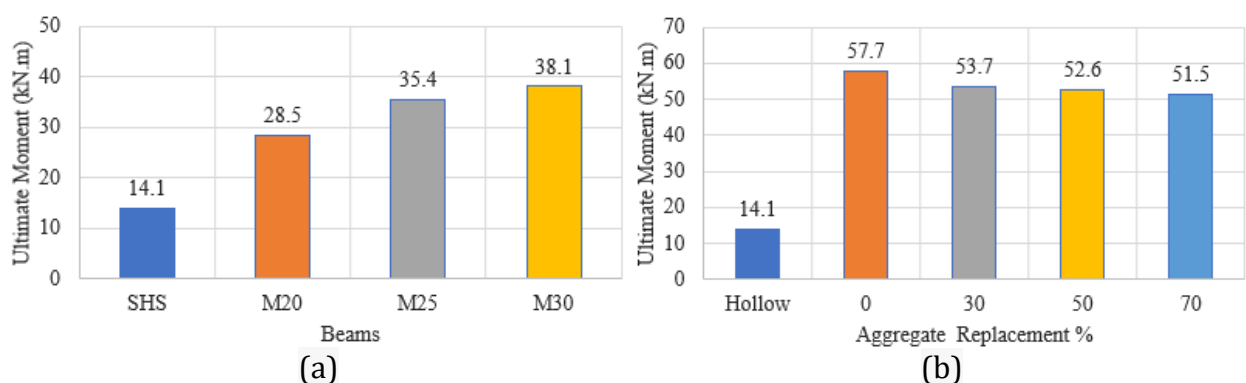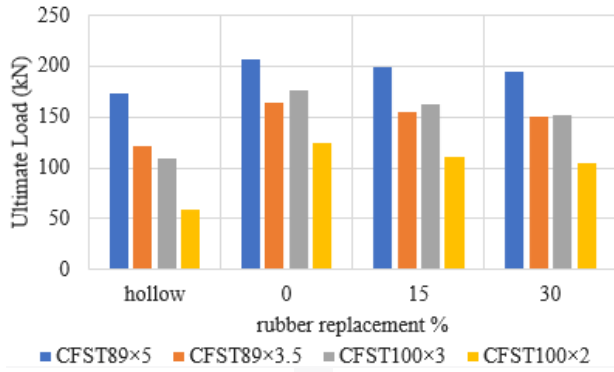
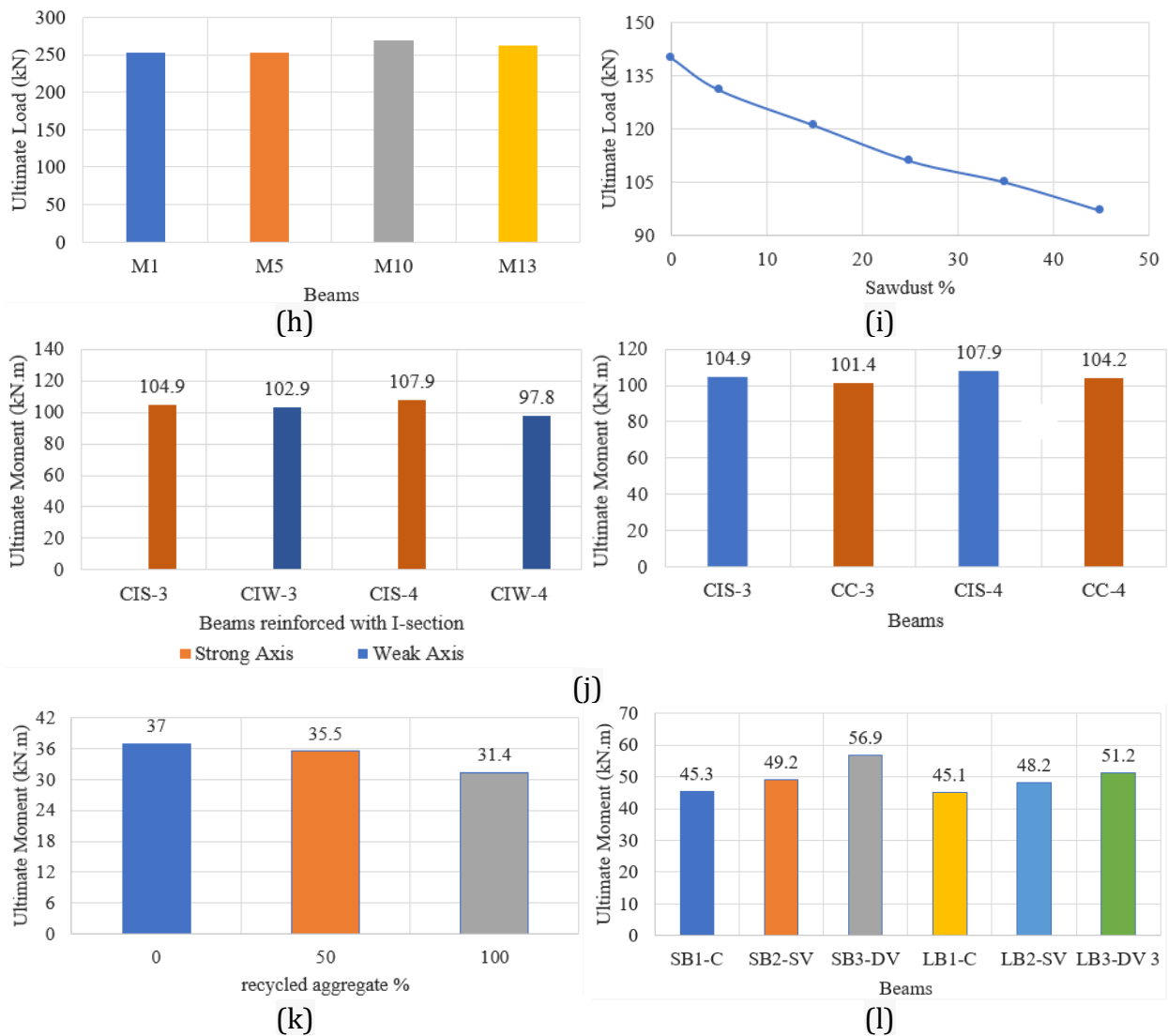(c)
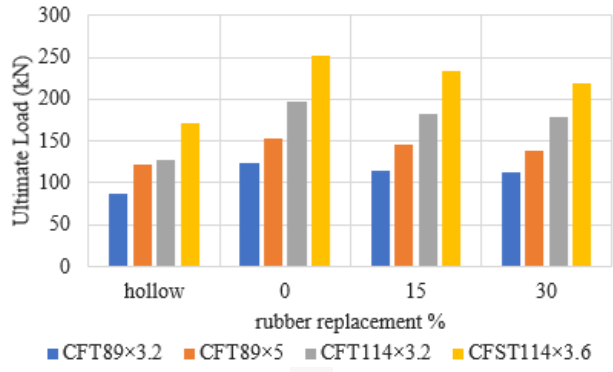
(d)

(e)

(f)

(g)

Figure 6. Moment and load capacity variation with different effects, **(a) (Pandian and Narayanan, 2023) (b) (Al Zand et al., 2021) (c) (Dong et al., 2019b) (d) (Dong et al., 2019a) (e) (Mujdeci et al., 2022) (f) (Al-Nini et al., 2020) (g) (Guler and Yavuz, 2019) (h) (Karuppanan and Vennila, 2020) (i) (Hanoon et al., 2023) (j) (Shi et al., 2020) (k) (Dabbagh et al., 2023) (l) (Al Zand et al., 2020).**

4.5 Ductility

One of the benefits of CFST beams is their great ductility. CFST beams can become even more ductile by using rubberized concrete, where ductility increases with a higher rubber replacement ratio **(Mujdeci et al., 2022)**. RuC, with greater ductility, exhibited a larger deformation capacity that effectively matched the shape of the steel tube's buckle, thus delaying the occurrence of buckling failure **(Dong et al., 2019a; 2019b)**. the ductile behavior of filling concrete can be enhanced by adding steel and hybrid fibers, which control the formation and propagation of cracks. Additionally, the presence of the filling concrete delayed local buckling and improved the ductility capacities. There is a significant increase in ductility values for steel and hybrid FRC-filled beams compared to plain concrete-filled beams. Hybrid-filled beams show a slight increase in moment capacity and ductility

compared to steel-filled **(Guler and Yavuz, 2019)**. **Figure 7** illustrates the variation in ductility in terms of ductility index (DI) and ductility factor under different conditions.
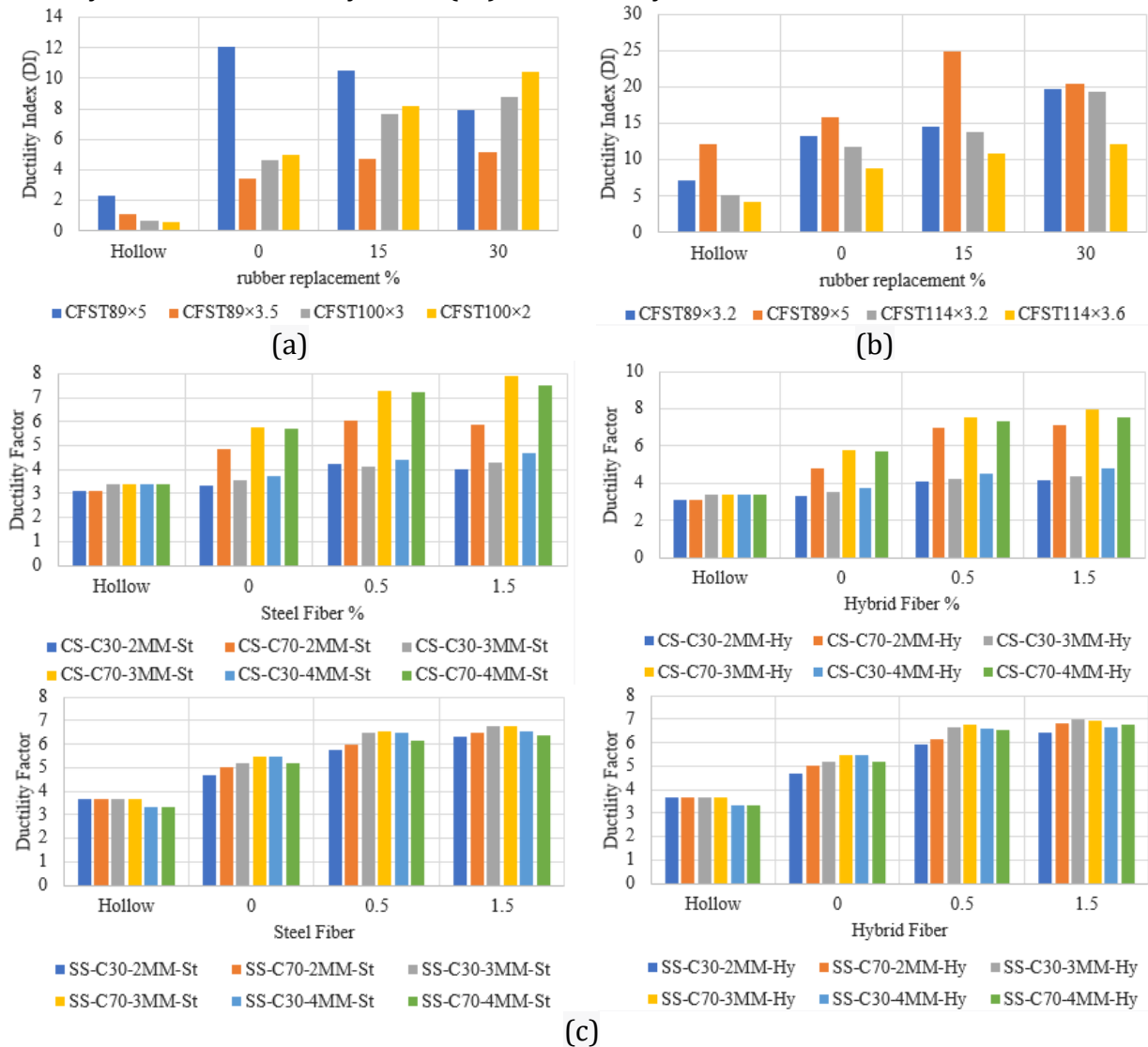

(a)   (b)

(c)

Figure 7. The variation of ductility in terms of ductility index and ductility factor with different effects, **(a) (Dong et al., 2019b) (b) (Dong et al., 2019a) (c) (Guler and Yavuz, 2019).**
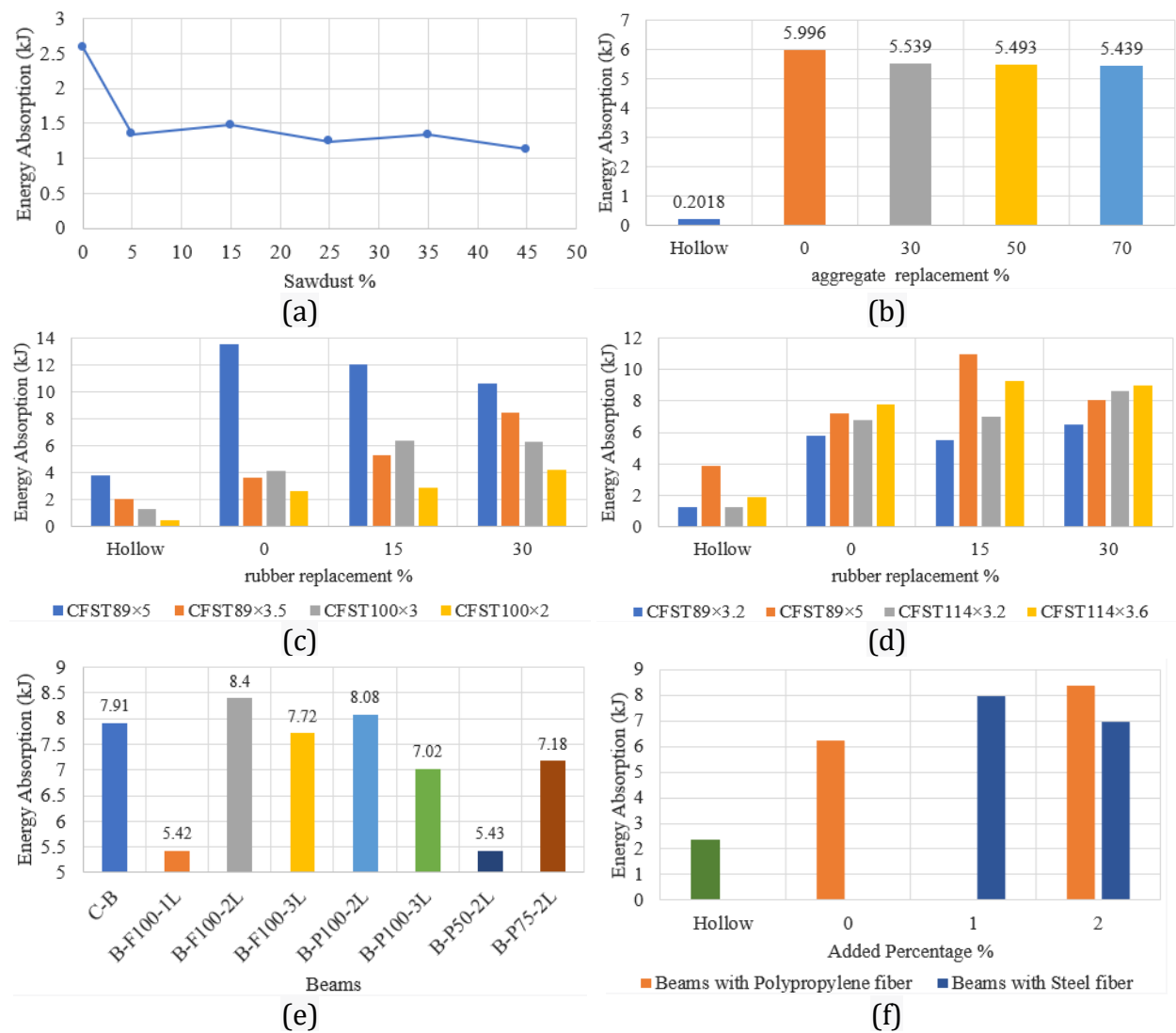
4.6 Energy Absorption

It is important to take a look at the energy absorption capability of a structure in order to assess load capacity. When a structural system faces environmental and unusual loads, ductility alone becomes insufficient for ensuring safety. Energy absorption reflects the structural strength of a system under unexpected loads. Numerous prior studies have shown that CFST beams are more efficient in energy dissipation compared to hollow beams. **(Hanoon et al., 2023)** found that the CFST beam with 0% sawdust had the highest energy absorption, while the specimen with 45% sawdust had the lowest energy absorption. The addition of sawdust reduced the enhancement ratio (43.22% to 56.52%) compared to CFST0 beam. This was confirmed by **(Al Zand et al., 2021)** with different aggregate replacements. It was observed that the energy absorption for a beam filled with normal concrete increased

29.7 times compared to the hollow section. However, this increase was reduced with higher aggregate replacements.

As section slenderness increased, energy absorption decreased due to the lowered load-carrying capacity. Higher rubber content enhanced deformation capacity and delayed steel tube failure, leading to greater energy absorption **(Dong et al., 2019a; 2019b)**. **(Al-Nini et al., 2020)** found that energy absorption changed with the number and wrapping extent of CFRP sheets. Toughness is a critical parameter representing the capacity of beams to absorb energy, as studied by **(Guler and Yavuz, 2019)**. it was found that hybrid fibers slightly outperformed steel fibers in enhancing toughness in most beams. Furthermore, the inclusion of polypropylene fiber, as explored by **(Karuppanan and Vennila, 2020)**, led to an overall improvement in energy absorption. **(Al Zand et al., 2020)** found that beams with double V-shaped grooves resulted in higher EA values compared to their corresponding samples. The EA increased by about 29.2%, while single V-shaped groove beams exhibited an increase of around 11.3%. **Figure 8** shows the variation of energy absorption under different conditions.
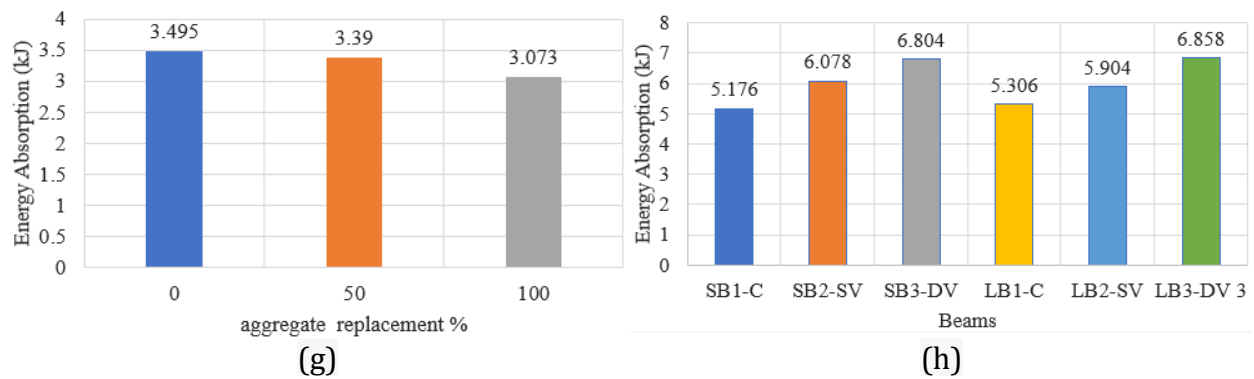

(a)

(b)

(c)

(d)

(e)

(f)

Figure 8. The variation of energy absorption with different effects, **(a) (Hanoon et al., 2023) (b) (Al Zand et al., 2021) (c) (Dong et al., 2019b) (d) (Dong et al., 2019a) (e) (Al-Nini et al., 2020) (f) (Karuppanan and Vennila, 2020) (g) (Dabbagh et al., 2023) (h) (Al Zand et al., 2020).**

5. CONCLUSIONS

This research provides an overview of CFST beams, summarizing findings on their properties and behavior, including geometry, concrete strength, failure modes, capacity, ductility, and energy absorption. The following conclusions can be inferred:

- Decreasing the D/t ratio enhances the composite section strength and improves the confinement of the concrete infill, which increases the concrete compressive strength and the overall load and moment-carrying capacity of the CFST beams.
- Increasing the L/D ratio reduces the ultimate load and moment capacity of CFST beams.
- The square cross-section for CFST beams has greater load and moment-carrying capacity than rectangular and circular sections and demonstrates less deformation.
- Increasing concrete compressive strength enhances both the CFST beam's ultimate load capacity and ductility, with ductility showing greater improvement than load capacity.
- While the deflection shape of the beam remained unchanged using CFRP sheets, it limits crack propagation and increases the CFST beam's load capacity and energy absorption, with greater effects when used with higher concrete strength and influenced by the CFRP configuration.
- CFST beams exhibit greater ductility than hollow beams, which can be further enhanced with rubberized concrete, particularly at higher rubber replacement ratios, as well as by incorporating steel and hybrid fibers that control crack formation and propagation; additionally, concrete infill improves ductility in slender tubes by delaying local buckling.
- CFST beams exhibited enhanced energy absorption capacity due to the presence of rubber in the concrete, which delayed steel tube failure, as well as the addition of steel and hybrid fibers; however, increasing the proportion of recycled aggregates in recycled CFST beams decreased energy absorption.

A gap in the existing literature was observed concerning beams with transverse openings for the installation of pipes and utility ducts required for various services.

NOMENCLATURE

Symbol	Description	Symbol	Description
CFRP	Carbon fiber reinforced polymer	Fcu	Compressive strength based on cubic samples
CFST	Concrete-filled steel tubes	LWC	lightweight concrete
CS	Carbon steel	NC	Normal concrete
DCLs	Demolished concrete lumps	Rcu	Rubberized concrete
f_c'	Concrete compressive strength based on cylinder samples	SS	Stainless steel

Acknowledgements

Credit Authorship Contribution Statement

All authors have read and approved the manuscript. Ali Mohammed drafted the original version and contributed to writing, reviewing, editing, validation, and software. Salah Al Zaidee reviewed and edited the manuscript, providing supervision, methodology, and support.

Declaration of Competing Interest

The authors declare that they have no known competing financial interests or personal relationships that could have appeared to influence the work reported in this paper.

REFERENCES

Abdeldaim, A.A., Mohamed, H. and Radhouane, M., 2020. Flexural performance of unbonded posttensioned rectangular concrete filled FRP tube beams. *Journal of Composites for Construction*, 24(5), P. 04020058. https://doi.org/10.1061/(ASCE)CC.1943-5614.0001063.

Abuzaid, O., Nabilah, A.B., Safiee, N.A. and Noor Azline, M.N., 2019. Rubberized concrete filled steel tube. *IOP Conference Series: Earth and Environmental Science*, 357(1), P. 012014. https://doi.org/10.1088/1755-1315/357/1/012014.

Alghossoon, A. and Varma, A., 2023. Rectangular filled composite members made from high strength materials: Behavior and design of columns and beams. *Thin-Walled Structures*, 185, P. 110641. https://doi.org/10.1016/j.tws.2023.110641.

Al-Nini, A., Nikbakht, E., Syamsir, A., Shafiq, N., Mohammed, B.S., Al-Fakih, A., Al-Nini, W. and Amran, Y.H.M., 2020. Flexural behavior of double-skin steel tube beams filled with fiber-reinforced cementitious composite and strengthened with CFRP sheets. *Materials*, 13(14). https://doi.org/10.3390/ma13143064.

Alqarni, M., Noman, A. and Bashir, M.A., 2019. Numerical simulation and parametric study on the moment capacity of composite beam. *Computational Engineering and Physical Modeling*, 2(3), pp.16–26. https://doi.org/10.22115/cepm.2019.199497.1069.

AL-Shaar, A.A.M. and Göğüş, M.T., 2018. Performance of retrofitted self-compacting concrete-filled steel tube beams using external steel plates. *Advances in Materials Science and Engineering*, 2018, P. 3284745. https://doi.org/10.1155/2018/3284745.

Alshimmeri, A.J.H., 2016. Structural behavior of confined concrete filled aluminum tubular (CFT) columns under concentric load. *Journal of Engineering*, 22(8), pp.125–139. https://doi.org/10.31026/j.eng.2016.08.08.

Al Zand, A.W., Badaruzzaman, W.H.W., Mutalib, A.A. and Hilo, S.J., 2018. Flexural behavior of CFST beams partially strengthened with unidirectional CFRP sheets: experimental and theoretical study. *Journal of Composites for Construction*, *22*(4), p.04018018. https://doi.org/10.1061/(ASCE)CC.1943-5614.0000852.

Arivalagan, S. and Kandasamy, S., 2010a. Finite element analysis on the flexural behaviour of concrete filled steel tube beams. *Journal of Theoretical and Applied Mechanics*, 48, pp.505–516.

Arivalagan, S. and Kandasamy, S., 2010b. Flexural and cyclic behaviour of hollow and concrete-filled steel tubes. *CCFSS Proceedings of International Specialty Conference on Cold-Formed Steel Structures (1971 - 2018)*, 5. https://scholarsmine.mst.edu/isccss/20iccfss/20iccfss-session5/5

Aslani, F., Gunawardena, Y. and Dehghani, A., 2019. Behaviour of concrete filled glass fibre-reinforced polymer tubes under static and flexural fatigue loading. *Construction and Building Materials*, [online] 212, pp.57–76. https://doi.org/10.1016/j.conbuildmat.2019.03.321.

Assi, I.M., Qudeimat, E.M. and Hunaiti, Y.M., 2003. Ultimate moment capacity of foamed and lightweight aggregate concrete-filled steel tubes. *Steel and Composite Structures, An International Journal*, 3(3), pp.199–212. https://doi.org/10.12989/scs.2003.3.3.199.

Aziz, R.J., Al-Hadithy, L.K. and Resen, S.M., 2016. Behavior of concrete filled double skin steel tubular columns under static axial compression load. *Journal of Engineering and Sustainable Development*, 20(2), pp.174–189.

Brown, N.K., Kowalsky, M.J. and Nau, J.M., 2015. Impact of D/t on seismic behavior of reinforced concrete filled steel tubes. *Journal of Constructional Steel Research*, 107, pp.111–123. https://doi.org/10.1016/j.jcsr.2015.01.013.

Chavan, M.K.U., Kadam, M.S.S. and Dr. Pise, C.P., 2021. Experimental study on flexural behavior of concrete filled steel tube beam. *International Journal of Engineering Research and Technology (IJERT)*, 10(1), pp.424–428.

Chen, D., Montano, V., Huo, L., Fan, S. and Song, G., 2020. Detection of subsurface voids in concrete-filled steel tubular (CFST) structure using percussion approach. *Construction and Building Materials*, 262, P. 119761. https://doi.org/10.1016/j.conbuildmat.2020.119761.

Chen, Y., Feng, R. and Wang, L., 2017. Flexural behaviour of concrete-filled stainless steel SHS and RHS tubes. *Engineering Structures*, 134, pp.159–171. https://doi.org/10.1016/j.engstruct.2016.12.035.

Dabbagh, N.M., Al Zand, A.W., Liejy, M.C., Ansari, M., Tawfeeq, W.M., Badaruzzaman, W.H., Kaish, A.B.M.A. and Yaseen, Z.M., 2023. Strengthening behavior of rectangular stainless steel tube beams filled with recycled concrete using flat cfrp sheets. *Buildings*, 13(4). https://doi.org/10.3390/buildings13041102.

Deng, Y., Norton, T.R. and Tuan, C.Y., 2013. Numerical analysis of concrete-filled circular steel tubes. *Proceedings of the Institution of Civil Engineers - Structures and Buildings*, 166(1), pp.3–14. https://doi.org/10.1680/stbu.11.00001.

Dexin, X., 2012. Structural behaviour of concrete filled steel tubes with high strength materials. *ScholarBank@NUS Repository*.

Dong, M., Elchalakani, M., Karrech, A., Fawzia, S., Mohamed Ali, M.S., Yang, B. and Xu, S.-Q., 2019a. Circular steel tubes filled with rubberised concrete under combined loading. *Journal of Constructional Steel Research*, 162, P. 105613. https://doi.org/10.1016/j.jcsr.2019.05.003.

Dong, M., Elchalakani, M., Karrech, A., Hassanein, M.F., Xie, T. and Yang, B., 2019b. Behaviour and design of rubberised concrete filled steel tubes under combined loading conditions. *Thin-Walled Structures*, 139, pp.24–38. https://doi.org/10.1016/j.tws.2019.02.031.

Du, Y., Gao, D., Chen, Z., Deng, X. and Qian, K., 2023. Experimental study on the flexural behavior of square high-strength concrete-filled steel tube beams with different CFRP wrapping schemes. *Composite Structures*, 304, P. 116325. https://doi.org/10.1016/j.compstruct.2022.116325.

Du, Z.L., Liu, Y.P., He, J.W. and Chan, S.L., 2019. Direct analysis method for noncompact and slender concrete-filled steel tube members. *Thin-Walled Structures*, 135, pp.173–184. https://doi.org/10.1016/j.tws.2018.11.007.

Elghazouli, A.Y., Mujdeci, A., Bompa, D. V and Guo, Y.T., 2022. Experimental cyclic response of rubberised concrete-filled steel tubes. *Journal of Constructional Steel Research*, 199, P. 107622. https://doi.org/10.1016/j.jcsr.2022.107622.

Eom, S.S., Vu, Q.V., Choi, J.H., Park, H.H. and Kim, S.E., 2019. Flexural behavior of concrete-filled double skin steel tubes with a joint. *Journal of Constructional Steel Research*, 155, pp. 260–272. https://doi.org/10.1016/j.jcsr.2018.12.012

Fahmi, H.M. and Tofeq, T., 2012. Fint element analysis of composite steel-concrete beams subjected to fire. *Al-Nahrain Journal for Engineering Sciences*, 15(1), pp.1–11. https://nahje.com/index.php/main/article/view/631

Farhan, K. and Shallal, M., 2020. Experimental behaviour of concrete-filled steel tube composite beams. *Archives of Civil Engineering*, 64, pp.235–251. https://doi.org/10.24425/ace.2020.131807.

Feng, R., Chen, Y., Wei, J., Huang, J., Huang, J. and He, K., 2018. Experimental and numerical investigations on flexural behaviour of CFRP reinforced concrete-filled stainless steel CHS tubes. *Engineering Structures*, 156, pp.305–321. https://doi.org/10.1016/j.engstruct.2017.11.032.

Flor, J., Fakury, R., Caldas, R., Rodrigues, F. and Araújo, A., 2017. Experimental study on the flexural behavior of large-scale rectangular concrete-filled steel tubular beams. *Revista IBRACON de Estruturas e Materiais*, 10, pp.895–905. https://doi.org/10.1590/s1983-41952017000400007.

Ghannam, S., 2016. Flexural strength of concrete-filled steel tubular beam with partial replacement of coarse aggregate by granite. *International Journal of Civil Engineering and Technology*, 7(5).

Gkantou, M., Georgantzia, E., Kadhim, A., Kamaris, G.S. and Sadique, M., 2023. Geopolymer concrete-filled aluminium alloy tubular cross-sections. *Structures*, 51, pp.528–543. https://doi.org/10.1016/j.istruc.2023.02.117.

Guler, S. and Yavuz, D., 2019. Post-cracking behavior of hybrid fiber-reinforced concrete-filled steel tube beams. *Construction and Building Materials*, 205, pp.285–305. https://doi.org/10.1016/j.conbuildmat.2019.01.192.

Han, L.H., 2004. Flexural behaviour of concrete-filled steel tubes. *Journal of Constructional Steel Research*, 60(2), pp.313–337. https://doi.org/10.1016/j.jcsr.2003.08.009.

Han, L.H., Li, W. and Bjorhovde, R., 2014. Developments and advanced applications of concrete-filled steel tubular (CFST) structures: Members. *Journal of Constructional Steel Research*, 100, pp.211–228. https://doi.org/10.1016/j.jcsr.2014.04.016.

Hanoon, A.N., Hason, M.M., Sharba, A.A.K., Abdulhameed, A.A., Amran, M., Avudaiappan, S. and Flores, E.S., 2023. Sawdust-based concrete composite-filled steel tube beams: an experimental and analytical investigation. *Journal of Composites Science*, 7(6). https://doi.org/10.3390/jcs7060256.

Hanoon, A.N., Al Zaidee, S.R., Banyhussan, Q.S. and Abdulhameed, A.A., 2018. Modified strut effectiveness factor for FRP-reinforced concrete deep beams. *International Journal of Engineering and Technology*, 7(4.20), pp.485–490.

Hassooni, A.N. and Al Zaidee, S.R., 2022. Behavior and strength of composite columns under the impact of uniaxial compression loading. *Engineering, Technology and Applied Science Research*, 12(4), pp.8843–8849. https://doi.org/10.48084/etasr.4753.

Hou, C.C., Han, L.H., Wang, Q.L. and Hou, C., 2016. Flexural behavior of circular concrete filled steel tubes (CFST) under sustained load and chloride corrosion. *Thin-Walled Structures*, 107, pp.182–196. https://doi.org/10.1016/j.tws.2016.02.020.

Ibrahim, A.M., Salman, W.D. and Bahlol, F.M., 2019. Flexural behavior of concrete composite beams with new steel tube section and different shear connectors. *Tikrit Journal of Engineering Sciences*, 26(1), pp.51–61. https://doi.org/10.25130/tjes.26.1.07.

Joseph, N., James, J. and Philip, P., 2016. Flexural performance of concrete filled steel tube beams. *International Journal of Engineering Research and Technology (IJERT)*, 05(07).

Karuppanan, K. and Vennila, G., 2020. Behaviour of hybrid fibre reinforced concrete-filled steel tubular beams and columns. *Matéria (Rio de Janeiro)*, 25, P. 12558. https://doi.org/10.1590/s1517-707620200001.0883.

Khalaf, S., Abed, F. and Alhoubi, Y., 2023. Flexural behavior of circular concrete filled steel tubes with partially incorporated demolished concrete lumps. *Composites Part C: Open Access*, 10, P. 100346. https://doi.org/10.1016/j.jcomc.2023.100346.

Li, G.C., Chen, B.W., Yang, Z.J., Liu, Y.P. and Feng, Y.H., 2021. Experimental and numerical behavior of eccentrically loaded square concrete-filled steel tubular long columns made of high-strength steel and concrete. *Thin-Walled Structures*, 159, P. 107289. https://doi.org/10.1016/j.tws.2020.107289.

Li, W., Chen, B., Han, L.H. and Lam, D., 2020. Experimental study on the performance of steel-concrete interfaces in circular concrete-filled double skin steel tube. *Thin-Walled Structures*, 149, P. 106660. https://doi.org/10.1016/j.tws.2020.106660.

Liu, D., Xia, Z., Wang, J. and Zuo, J., 2021. Flexural strengthening mechanism of concrete-filled steel tube beam by welding round steel at soffit of the beam. *Structures*, 34, pp. 2243–2261. https://doi.org/10.1016/j.istruc.2021.08.081.

Liu, D., Zuo, J., Wang, J., Li, P., Duan, K., Zhang, D. and Guo, S., 2019. Bending failure mechanism and strengthening of concrete-filled steel tubular support. *Engineering Structures*, 198, P. 109449. https://doi.org/10.1016/j.engstruct.2019.109449.

Lu, H., Han, L.H. and Zhao, X.L., 2009. Analytical behavior of circular concrete-filled thin-walled steel tubes subjected to bending. *Thin-Walled Structures*, 47(3), pp. 346–358. https://doi.org/10.1016/j.tws.2008.07.004.

Mahdi, H.H. and Shallal, M.A., 2021. The effect of filling materials on the behaviour of filled steel tube composite beam. *Journal of Physics: Conference Series*, 1895(1), P. 012057. https://doi.org/10.1088/1742-6596/1895/1/012057.

Mohammed, S.N. and Mohsen, M.H., 2014. The effective width in composite steel concrete beams at ultimate loads. *Journal of Engineering*, 20(8). https://doi.org/10.31026/j.eng.2014.08.01.

Mujdeci, A., Bompa, D. V and Elghazouli, A.Y., 2021. Confinement effects for rubberised concrete in tubular steel cross-sections under combined loading. *Archives of Civil and Mechanical Engineering*, 21(2), P. 53. https://doi.org/10.1007/s43452-021-00204-8.

Mujdeci, A., Guo, Y.T., Bompa, D. V and Elghazouli, A.Y., 2022. Axial and bending behaviour of steel tubes infilled with rubberised concrete. *Thin-Walled Structures*, 181, P. 110125. https://doi.org/10.1016/j.tws.2022.110125.

Nguyen, T.T., Nguyen, V.B. and Thai, M.Q., 2023. Flexural strength of partially concrete-filled steel tubes subjected to lateral loads by experimental testing and finite element modelling. *Buildings*, 13(1). https://doi.org/10.3390/buildings13010216.

Nimisha A, R. and Abhilasha P, S., 2019. Analysis of concrete filled steel tubular beams. *International Journal of Scientific and Engineering Research*, 10(5), pp.308–312.

Ou, J., Shao, Y., Huang, C., Chen, Y. and Bi, X., 2023. Flexural behavior of circular concrete filled steel tubular members strengthened by CFRP sheets. *Structures*, 55, pp.201–214. https://doi.org/10.1016/j.istruc.2023.06.031.

Pandian, M. and Narayanan, M., 2023. Experimental investigation on concrete – filled steel tubular beam. *AIP Conference Proceedings*, 2766(1), p.020058. https://doi.org/10.1063/5.0139792.

Prion, H.G.L. and Boehme, J., 1994. Beam-column behaviour of steel tubes filled with high strength concrete. *Canadian Journal of Civil Engineering*, 21(2), pp.207–218. https://doi.org/10.1139/l94-024.

Saini, D. and Shafei, B., 2019. Investigation of concrete-filled steel tube beams strengthened with CFRP against impact loads. *Composite Structures*, 208, pp.744–757. https://doi.org/10.1016/j.compstruct.2018.09.057.

Shi, Y.L., Xian, W., Wang, W.D. and Li, H.W., 2020. Mechanical behaviour of circular steel-reinforced concrete-filled steel tubular members under pure bending loads. *Structures*, 25, pp.8–23. https://doi.org/10.1016/j.istruc.2020.02.017.

Tahir, A.K. and Shallal, M.A., 2021. Experimental study of concrete filled steel tube composite beam under hogging moment. *IOP Conference Series: Materials Science and Engineering*, 1090(1), P. 012062. https://doi.org/10.1088/1757-899X/1090/1/012062.

Wang, W.D., Han, L.H. and Zhao, X.L., 2009. Analytical behavior of frames with steel beams to concrete-filled steel tubular column. *Journal of Constructional Steel Research*, 65(3), pp.497–508. https://doi.org/10.1016/j.jcsr.2008.11.002.

Wu, F., Zeng, Y., Li, B. and Lyu, X., 2021. Experimental investigation of flexural behavior of ultra-high-performance concrete with coarse aggregate-filled steel tubes. *Materials*, 14(21). https://doi.org/10.3390/ma14216354.

Wu, H., Ren, G.M., Fang, Q. and Liu, J.Z., 2019. Response of ultra-high performance cementitious composites filled steel tube (UHPCC-FST) subjected to low-velocity impact. *Thin-Walled Structures*, 144, P. 106341. https://doi.org/10.1016/j.tws.2019.106341.

Xian, W., Wang, W.D., Wang, R., Chen, W. and Hao, H., 2020. Dynamic response of steel-reinforced concrete-filled circular steel tubular members under lateral impact loads. *Thin-Walled Structures*, 151, P. 106736. https://doi.org/10.1016/j.tws.2020.106736.

Xiong, M.X., Xiong, D.X. and Liew, J.Y.R., 2017. Flexural performance of concrete filled tubes with high tensile steel and ultra-high strength concrete. *Journal of Constructional Steel Research*, 132, pp.191–202. https://doi.org/10.1016/j.jcsr.2017.01.017.

Xu, J., Wang, Y., Ren, R., Wu, Z. and Ozbakkaloglu, T., 2020. Performance evaluation of recycled aggregate concrete-filled steel tubes under different loading conditions: Database analysis and modelling. *Journal of Building Engineering*, 30, P. 101308. https://doi.org/10.1016/j.jobe.2020.101308.

Yang, Y.F., Zhang, Z.C. and Fu, F., 2015. Experimental and numerical study on square RACFST members under lateral impact loading. *Journal of Constructional Steel Research*, 111, pp.43–56. https://doi.org/10.1016/j.jcsr.2015.04.004.

Al Zand, A.W., Ali, M.M., Al-Ameri, R., Badaruzzaman, W.H., Tawfeeq, W.M., Hosseinpour, E. and Yaseen, Z.M., 2021. Flexural strength of internally stiffened tubular steel beam filled with recycled concrete materials. *Materials*, 14(21). https://doi.org/10.3390/ma14216334.

Al Zand, A.W., Badaruzzaman, W.H.W., Al-Shaikhli, M.S. and Ali, M.M., 2020. Flexural performance of square concrete-filled steel tube beams stiffened with V-shaped grooves. *Journal of Constructional Steel Research*, 166, P. 105930. https://doi.org/10.1016/j.jcsr.2020.105930.

Al Zand, A.W., Badaruzzaman, W.H.W. and Tawfeeq, W.M., 2020. New empirical methods for predicting flexural capacity and stiffness of CFST beam. *Journal of Constructional Steel Research*, 164, P. 105778. https://doi.org/10.1016/j.jcsr.2019.105778.

Zhan, Y., Zhao, R., Ma, Z.J., Xu, T. and Song, R., 2016. Behavior of prestressed concrete-filled steel tube (CFST) beam. *Engineering Structures*, 122, pp. 144–155. https://doi.org/10.1016/j.engstruct.2016.04.050.

Zhang, W.F., Gardner, L., Wadee, M.A., Chen, K.S. and Zhao, W.Y., 2022a. On the uniform torsional rigidity of square concrete-filled steel tubular (CFST) sections. *Structures*, 43, pp.249–256. https://doi.org/10.1016/j.istruc.2022.06.046.

Zhang, Z.Y., Sun, Q., Wang, J.Q., Zhao, C., Zhao, B.Z. and Wang, J.T., 2022b. Experimental and analytical research on flexural behavior of concrete-filled high-strength steel tubular members. *Materials*, 15(11). https://doi.org/10.3390/ma15113790.

Zhou, Z., Denavit, M.D. and Zhou, X., 2023. New cross-sectional slenderness limits for stiffened rectangular concrete-filled steel tubes. *Engineering Structures*, 280, P. 115689. https://doi.org/10.1016/j.engstruct.2023.115689.

Zhu, X., Kang, M., Fei, Y., Zhang, Q. and Wang, R., 2021. Impact behavior of concrete-filled steel tube with cruciform reinforcing steel under lateral impact load. *Engineering Structures*, 247, P. 113104.

دراسة عملية وعددية للعتبات الانبوبية الفولاذية المملوءة بالخرسانة: بحث مراجعة

علي محمد عبد الرضا*، صلاح رحيمة عبيد

قسم الهندسة المدنية، كلية الهندسة، جامعة بغداد، بغداد، العراق

الخلاصة

أنابيب الفولاذ المملوءة بالخرسانة (CFST) هي عناصر انشائية مصنوعة من أنابيب مجوفة مملوءة بالخرسانة. الأنبوب الفولاذي والخرسانة يتعاونان لتوفير ميزة كبيرة. تعزز الخرسانة الأنبوب الفولاذي ضد الالتواء المحلي، بينما يوفر الأنبوب الفولاذي احتواءً للخرسانة مما يؤدي إلى زيادة كبيرة في قوة الخرسانة. زاد استخدام العتبات المملوءة بالخرسانة في المباني العالية بسبب خصائصها الميكانيكية الرائعة. لقد جذبت العتبات المملوءة بالخرسانة اهتمام الباحثين بسبب مرونتها العالية وصلابتها وقوتها وقدرتها على تحمل الانثناء بالمقارنة مع مقاطع الفولاذ الفارغة. تم تحسين العتبات المملوءة بالخرسانة بواسطة عدة طرق، بما في ذلك لفائف الألياف الكربونية المقواة بالبوليمر، وإضافة لوحة فولاذية خارجية، واستخدام الركام المعاد تدويره. بالإضافة إلى ذلك، تم تحسين الخرسانة عن طريق إضافة الألياف الفولاذية والاصطناعية. يغطي هذا مقال المراجعة البحوث التي تم إجراؤها على عتبات الأنابيب المملوءة بالخرسانة منذ عام 2019. يوفر الملخص نظرة عامة على ما قام به الباحثون من دراسات واكتشافات، وعلى ما يحتاج لمزيد من البحث.

الكلمات المفتاحية: أنابيب الفولاذ المملوءة بالخرسانة، CFST، عتبات مركبة، حبسمركبة، حبس، طور الفشل.